TRANSCRIPTIONAL MODULATION OF APOPTOSIS REGULATORS BY ROSCOVITINE AND RELATED COMPOUNDS

Xènia Garrofé-Ochoa, Ana M. Cosialls, Judit Ribas, Joan Gil and Jacint Boix

Molecular Pharmacology Group, Departament de Medicina Experimental, IRBLLEIDA-Universitat de Lleida, Catalunya, Spain (X.Garrofé-Ochoa, J. Ribas and J. Boix)

Departament de Ciències Fisiològiques II, IDIBELL-Universitat de Barcelona, Campus de Bellvitge, L'Hospitalet de Llobregat, Catalunya, Spain (A.M. Cosialls and J. Gil)

Corresponding author

Jacint Boix MD PhD

Molecular Pharmacology Group, Departament de Medicina Experimental, IRBLLEIDA-Universitat de Lleida, C/ Montserrat Roig 2, E-25008 Lleida, Catalunya, Spain.

Tel: +34 973702404, FAX: +34 973702426, E-mail: jacint.boix@mex.udl.cat

Footnotes

X.Garrofé-Ochoa and A.M. Cosialls contributed equally to this work.

J.Gil and J.Boix share the senior co-authorship.

Abstract

Chemical inhibitors of cyclin-dependent kinase (CDK), like roscovitine, are promising drugs in the context of new cancer therapies. Roscovitine and related compounds, like seliciclib and olomoucine, are effective inducers of apoptosis in many proliferating cells in culture. These compounds are known to activate the intrinsic or mitochondrial pathway of apoptosis. In order to better characterize this intrinsic pathway, a transcriptional analysis was performed using the reverse transcriptase-multiplex ligation-dependent probe amplification procedure (RT-MLPA). In five cell lines, we detected an early and marked reduction of most transcripts, which is consistent with the disruption of transcription that results from the inhibition of CDK7 and CDK9. However, the mRNA of *p53-upregulated modulator of apoptosis (PUMA)* gene escaped from this transcription inhibition in neuroblastoma cells with a functional p53 protein. The increase of *PUMA* mRNA was not found in roscovitine-treated cell lines defective in p53, which underwent apoptosis like their p53 proficient counterparts. In addition, in SH-SY5Y cells, sublethal and lethal concentrations of roscovitine produced equivalent increases of *PUMA* mRNA and protein. In conclusion, the increased expression of *PUMA* was not associated with apoptosis induction. On the contrary, mRNA and protein depletion of *MCL-1* gene correlated the best with cell demise. Moreover, NOXA protein suffered a far minor decrease than MCL-1. Because of the selective neutralization of NOXA by MCL-1, we hypothesize that the disruption of this balance is a critical event in apoptosis induction by roscovitine and related compounds.

Keywords

Roscovitine / Olomoucine / Seliciclib / RT-MLPA / BCL-2 family / p53

Introduction

The 2,6,9-trisubstituted purine chemistry defines a family of drugs characterized by being inhibitors of cyclin-dependent kinase (CDK) [1]. Roscovitine is the most extensively investigated compound in the family. For instance, only in year 2010, roscovitine has been studied in 79 original publications (reviews excluded), as revealed by means of a PubMed search. The pharmacology of roscovitine focused on cancer application has been recently reviewed in detail [2]. Furthermore, seliciclib, the (R) enantiomer of roscovitine is in clinical phases of development for cancer treatment [3, 4]. These facts notwithstanding, new roscovitine derivatives continue to be sought in order to improve the pharmacological profile of roscovitine [5, 6]. Olomoucine is also a 2,6,9-trisubstituted purine [1]. Olomoucine displays lower pharmacological potency than roscovitine but a similar, though not identical, activity profile [7]. Interestingly, olomoucine has an inactive isomer, named iso-olomoucine that becomes the ideal negative control for biological experiments [8, 9].

In addition to cancer, other diseases such as retroviral infections, protozoal parasitosis, proliferative glomerulonephritis or several types of neurodegeneration have been regarded as possible applications for roscovitine [1]. Moreover, by apoptosis induction in neutrophils, roscovitine potential as an anti-inflammatory drug is being investigated [10]. In this therapeutic context, roscovitine is known to act paradoxically. Roscovitine triggers apoptosis in many tumor cells [2] but prevents it in other experimental paradigms [11, 12]. A satisfactory explanation for these opposing results is lacking, but a proposal to conciliate them will be further discussed.

We have focused our research on the apoptotic mode of action of roscovitine and olomoucine. Initially, we characterized their effects on SH-SY5Y, a tumor cell line derived from human neuroblastoma. We characterized the time course and concentration dependency of the process [9]. In SH-SY5Y cells, we discarded the involvement of an extrinsic pathway [13]. Furthermore, we showed these drugs to activate BAX protein and to trigger a mitochondrial or intrinsic pathway [14]. Intriguingly, enforced expression of BCL-2 and BCL-X_L proteins in SH-SY5Y

cells had provided no apoptotic protection against roscovitine and olomoucine [9]. The neutralization of BCL-2 and BCL-X_L antiapoptotic effects by this type of compounds remained to be explained in our cell model. In order to investigate this issue, we decided to characterize the gene expression of several regulators of the intrinsic pathway. The RT-MLPA technique was chosen as our analytical tool. This procedure allowed the simultaneous quantification of the mRNA expressed from several genes involved in apoptosis execution and regulation [15, 16]. Our approach revealed that the expression of one p53-regulated gene, *PUMA*, increased while the others in the test were repressed by the action of roscovitine and related compounds. The translation into protein of the most significant mRNA variations was assessed and agreed in most instances. Taking together our results, we envisage a complex scenario where the balance of some elements integrating the intrinsic pathway, particularly NOXA and MCL-1, are determining if apoptosis will occur.

Materials and methods

Chemical reagents and primary antibodies

Roscovitine, olomoucine, iso-olomoucin, pifithrin-α (Pft-α) and cyclic pifithrin-α (cPft-α) were acquired from Calbiochem (San Diego, CA, USA). Seliciclib (R-rosccovitine or CYC202) was kindly supplied by Prof. L. Meijer (Station Biologique de Roscoff, CNRS, France). Anti-BCL-2 monoclonal antibody (Dakocytomation, Glostrup, Denmark) was used at a dilution 1:1000. Anti-BCL-X_L polyclonal antibody (BD-Biosciences, San Diego, CA, USA) was employed at a dilution 1:2000. The working dilution for anti-MCL-1 polyclonal antibody from Sigma (St. Louis, MO, USA) and anti-p53 monoclonal antibody from Upstate (Lake Placid, NY, USA) was 1:4000. Analogously, 1:500 was used for anti-NOXA monoclonal antibody (Abcam, Cambridge, UK) and 1:1000 for anti-PUMA polyclonal antibody (Cell Signaling Technologies, Danvers, MA, USA). Glyceraldehyde-3-P-dehydrogenase (GAPDH) was detected directly with a peroxidase-conjugated monoclonal antibody from Sigma. This monoclonal antibody was employed at 1:4000 and its purpose was to assess the

protein load per lane in Western blots and densitometry quantifications. Unless otherwise stated, the non-listed reagents were from Sigma.

Cell culture and drug treatments

SH-SY5Y, Jurkat and HL-60 cells lines were obtained from the American Type Culture Collection (Manassas, VA, USA). IMR-5 and IMR-32 are two cell lines derived from human neuroblastoma, which origin and characterization have been reported before [17, 18]. The cell lines derived from neuroblastoma were grown in 2 mM L-glutamine supplemented DMEM media (Invitrogen, Barcelona, Spain) plus a 10% volume of FCS (Invitrogen). HL-60 and Jurkat cell lines were grown in RPMI media (Invitrogen) plus a 10% volume of FCS. All media contained Plasmocin™ (InvivoGen, San Diego, CA, USA) as the only antibiotic and its concentration was 5µg/ml. General culturing conditions were 37°C and a water-saturated, 5% CO_2 atmosphere. Stock solutions of roscovitine and the other chemical reagents were prepared in DMSO. From these stock solutions, drugs were delivered to the culture media and adjusted to the final concentrations reported in the text and figures. The serial dilution procedure was used in concentration-dependency determinations.

Cell death and apoptosis assessment

In order to quantify the ratios of cell death in the culture plates, the Cell Titer 96® and Cytotox 96® kits were used. Cell Titer 96® allowed to assess the reduction of 3-(4,5-dimethylthiazol-2-yl)-5-(3-carboxy methoxyphenyl)-2-(4-sulfophenyl)-2H-tetrazolium, inner salt (MTS). Cytotox 96® measured the amount of lactate deshydrogenase (LDH) released from dying cells. Both kits were provided by Promega Biotech Ibérica, SL (Barcelona, Spain) and used as we have previously reported [9]. Alternatively, Trypan blue staining and microscopic counts were also performed. Apoptosis was assessed by two procedures, bisBenzimide/Hoechst 33342 staining of chromatin plus fluorescence microscopy and the activation of DEVD targeted caspases [13].

RT-MLPA analysis

Cultured cells, either treated or untreated, were first washed with PBS and total RNA was extracted from the pellets. For this purpose, the RNeasy® kit was used according to the supplier instructions (Qiagen Inc, Valencia, CA, USA). Total RNA concentration was determined in a NanoDrop spectrophotometer (NanoDrop Technologies, Wilmington, DE, USA) and its integrity checked by a standard electrophoresis in agarose gels. Then, RNA samples were subjected to reverse transcriptase multiplex ligation–dependent probe amplification (RT-MLPA). The SALSA MLPA kit R011-Apoptosis-mRNA from MRC-Holland (Amsterdam, The Netherlands) was used. This procedure allows the simultaneous detection of 37 mRNA molecules, including the probes for mRNAs of 32 apoptosis-related proteins. In brief, a gene-specific probe mix was used to reverse transcribe 200 ng of total RNA. The resulting cDNA was annealed overnight at 60°C to the MLPA probe mix. Annealed oligonucleotides were ligated by adding Ligase-65 (MRC-Holland, Amsterdam) and incubation at 54°C for 15 minutes. Ligation products were amplified by PCR (35 cycles, 30 seconds at 95°C; 30 seconds at 60°C, and 1 minute at 72°C) with one unlabeled and one fluorescence labeled primer. The amplified PCR fragments were separated by capillary electrophoresis on a 48-capillary ABI-Prism 3730 Genetic Analyzer from Applied Biosystems/Hitachi (Foster City, CA, USA). Peak area was measured using GeneScan analysis software (Applied Biosystems). The levels of mRNA for each gene were expressed as a normalized ratio of the peak area divided by the peak area of an internal standard, a housekeeping gene of reference. Precisely, *β2-MICROGLOBULIN* for SH-SY5Y and *β-GLUCURONIDASE* for Jurkat, HL60, IMR-5 and IMR-32 cells. Therefore, the relative mRNA content of the genes of interest was calculated as a percentage (Supplemental Fig. 1, 3 and 4). In several diagrams (Fig. 1 to 4), the base-2 logarithm of the fold induction relative to untreated cells was calculated. This equalized to zero the mRNA content of the untreated conditions.

Western blot analysis

Cultured cells, either treated or untreated, were washed with PBS and proteins extracted from the pellets by a brief sonication in a buffer containing 100 mM Tris-HCl (pH 7.5), 1 mM EDTA, 1 mM PMSF, 2 μg/ml aprotinin, 1 μg/ml leupeptin and 2% SDS. After boiling for 5 minutes and a centrifugation at 12000g for 15 minutes, supernatants were collected and their protein content assessed by the NanoDrop spectrophotometer, mentioned above. Equal amounts of protein were loaded per lane in SDS 10, 12 or 15% polyacrylamide gel electrophoresis depending on the protein subjected to analysis. Then, proteins were transferred to Immobilon-P™ membranes (Millipore Iberica, Madrid, Spain) by means of a MINI® trans-blot module from Bio-Rad (Hercules, CA, USA). Membranes were reacted with the primary antibodies described above. Immunoblots were finally developed with the appropriate peroxidase-conjugated secondary antibody from Sigma and Immobilon™ Western detection reagent from Millipore. Chemiluminiscence was recorded and densitometries performed by means of a Chemidoc™ XRS system and the Quantity One (version 4.6) software from Bio-Rad. Peak intensity from each band of interest was normalized by the peak intensity of GAPDH in the same lane and then referred to analogous values from untreated cells. Data were finally translated into base-2 logarithms in order to homogenize these diagrams with those of the RT-MLPA analysis. As in those diagrams, values from the untreated condition became equalized to zero and, therefore, the bars representing the control value disappeared from the graph.

Results

Effects of roscovitine and related compounds on the expression of apoptotic regulators in cell lines derived from neuroblastoma

The main purpose of this report was to characterize the expression of genes regulating apoptosis in our experimental paradigms by means of the RT-MLPA procedure. Unless otherwise stated, SH-

SY5Y cells were treated with 50 μM roscovitine. We have determined this to be the standard concentration to induce apoptosis in most of the cell population at 48 hours of treatment [9]. Total RNA was extracted after 6 hours of treatment, a time characterized by a minimal activation of effector caspases (DEVDase activity) and extensive integrity of the cells [9, 13]. In order to check the effect of the drugs, control cultures were run in parallel and cell death was tested after 48 hours of treatment. At this time Trypan Blue and LDH release procedures confirmed that death was occurring in most of the cell population, as expected. The extracted RNA was then subjected to RT-MLPA analysis. Data were plotted into two types of bar diagrams (Fig. 1 and supplemental Fig. 1). In Fig. 1, bar value is the fold mRNA content has changed in treated versus untreated cells and, the number, is expressed as a base-2 logarithm (log_2). This type of graph emphasizes the changes produced by the drug treatment. In supplemental Fig. 1, bar value is the mRNA content expressed as the percentage (%) for each gene fragment in the final mixture of fragments that result from RT-MLPA. This type of graph preserves the information about the amount of expression for each gene in the cell line. The type of graph notwithstanding, similar conclusions could be drawn: a marked reduction for most of the mRNA studied. However, one exception emerged. Roscovitine treatment was increasing the mRNA of the BH3-only protein PUMA, on average, 4 times.

Next we tested other compounds related to roscovitine, precisely olomoucine and seliciclib in one experiment. At the concentrations employed, these compounds induce ratios and kinetics of cell apoptosis equivalent to those of roscovitine [9, 19]. RT-MLPA analysis was performed and controlled as described before. The results were analogous to those previously obtained with roscovitine as these compounds caused a general decrease of most mRNAs and an increase of *PUMA* that averaged 4 folds (Fig. 2A). In the same experiment, iso-olomoucine was tested (white bars in Fig. 2A). As expected, the profile generated by iso-olomoucine differed little from the one of untreated SH-SY5Y cells. Iso-olomoucine does not inhibit CDK at this concentration, does not cause cell death and becomes a good negative control of the experiment. Iso-olomoucine could have identified off-

target effects of the 2,6,9-trisubstituted purines on the expression of the genes studied by the RT-MLPA procedure.

In order to generalize these data to other cell lines, in one experiment we tested the effect of roscovitine on IMR-5 and IMR-32. Both cell lines are derived from human neuroblastoma. In these cell lines, we had previously studied the apoptotic effect of roscovitine and found to occur within a range of concentrations analogous to the one reported for SH-SY5Y [19]. Therefore, IMR-5 and IMR-32 cells were subjected to a treatment with 50 μM roscovitine for 6 hours. Cell death and RNA integrity were checked and, finally, RT-MLPA analysis was performed (Fig. 2B). The results displayed a great homology to those previously found in SH-SY5Y cells.

Roscovitine-induced increase of *PUMA* mRNA was dependent on p53.

PUMA is a BH3-only protein and its mRNA transcription is regulated by p53 [20, 21]. Neuroblastoma is a type of tumor characterized by maintaining a functional p53 protein, as we have observed in the three cell lines mentioned above [19]. Consequently, we questioned the involvement of p53 in the increase of *PUMA* mRNA caused by roscovitine. To first approach this issue, we thought of performing RT-MLPA analyses in cell lines known for being defective in p53. We chose HL-60 and Jurkat cell lines [22, 23]. HL-60 cells are derived from human promyelocytic leukemia and Jurkat cells, from human T cell leukemia. Since we had no previous characterization of the effects of roscovitine on these cell lines, we proceeded to characterize the concentration dependency of cell death by the MTS reduction (Fig. 3A) and the LDH release procedure (Fig. 3B). The range of death inducing concentrations did not differ from the one observed in the neuroblastoma cell lines. In addition, the type of cell death was characterized and found to be apoptotic based on the activation of effector caspases (Fig. 3C) and the nuclear morphology after bisBenzimide staining of chromatin (Supplemental Fig. 2). Finally, in one experiment, HL-60 (Supplemental Fig. 3) and Jurkat cells (Supplemental Fig. 4) were treated with roscovitine (50 μM) for 6 hours and the RT-MLPA analysis

was performed. Again, a marked reduction in the content of most mRNAs was detected (Fig. 3D). Interestingly, roscovitine did not cause *PUMA* mRNA increase in these cell lines defective in p53. In conclusion, neither p53 nor PUMA mRNA increase were necessary for apoptosis to occur in these cell lines.

To further explore this issue, in one experiment, we decided to use Pft-α and cPft-α. Both compounds are known for their ability to inhibit the transcriptional activity of p53 [24]. In SH-SY5Y cells, both compounds had a negligible effect on *PUMA* mRNA when used alone. However, both reversed the increase of *PUMA* mRNA caused by roscovitine in these cells. Moreover, we observed the mRNA to decrease (Fig. 4A), as previously observed in the HL-60 and Jurkat cell lines (Fig. 3D). Next we tested if Pft-α and cPft-α had any effect on the death ratios caused by roscovitine in SH-SY5Y cells. We found neither compound modified the death ratios (Fig. 4B). In conclusion, the increase of *PUMA* mRNA was an event that was being sustained by the transcriptional activity of p53 in SH-SY5Y cells treated with roscovitine. Furthermore, the increase of *PUMA* mRNA was not an event necessary for roscovitine to trigger apoptosis in these cells.

A prominent reduction in MCL-1 expression correlated with apoptosis induction by roscovitine

In our previous studies, we had determined 10 μM to be a sublethal concentration for roscovitine after 48 hours of treatment [9, 19]. We wondered what the RT-MLPA comparison of a sublethal versus a lethal concentration of roscovitine could uncover. Therefore, in one experiment, SH-SY5Y cells were treated for 6 hours with roscovitine at sublethal (10 μM) or lethal (50 μM) concentrations and RT-MLPA was performed (Fig. 4C). Surprisingly, the RT-MLPA profile was quite similar when the sublethal and lethal conditions were compared. Most mRNAs were reduced in the sublethal condition. Therefore, the roscovitine-induced disruption of transcription was already detectable at a concentration 10 μM. Similarly, the increase of PUMA mRNA was also observed in the sublethal

paradigm. This fact reinforced previous evidences about a non-essential role for the increase of PUMA mRNA in the cell death process. The only significant differences were observed in the mRNA content of the *BCL-2-like* genes. Lethal concentrations of roscovitine caused a greater reduction of *BCL-2*, *BCL-W*, *BCL-X$_L$* and *MCL-1* mRNAs than sublethal ones. The most manifest decay was observed in the content of *MCL-1* mRNA. This event correlated the best with apoptosis induction triggered by roscovitine in SH-SY5Y cells.

Protein content modifications associated with the roscovitine treatment

Since the mRNA content does not necessarily correlate with the protein one, we decided to validate some of the RT-MLPA results by Western blot (Supplemental Fig. 5), densitometric analysis and quantification, as reported in the methods section. In addition we used a time course approach to better characterize the phenomena. Initially, we focused on p53 protein and two of their downstream regulated targets, the BH-3-only proteins NOXA and PUMA (Fig. 5). Lethal concentrations stabilized p53 protein to a greater extent or, alternatively, with a faster kinetics than sublethal ones. NOXA is a BH3-only protein that preferentially binds and becomes neutralized by MCL-1 [25]. Accordingly, it was a good candidate to participate in the mechanism of apoptosis triggered by Roscovitine. *NOXA* mRNA experienced a small increase in the sublethal condition and a clear decrease in the lethal one (Fig. 4C). NOXA protein mimicked the behavior of the mRNA and, consequently, no clear correlation with cell death could be initially established.

Concerning PUMA protein, four isoforms (α, β, γ and δ) are possible and known to be the consequence of differential splicing [21]. However, only α and β isoforms are truly BH3-only proteins, displaying one BH3 domain and being involved in triggering the intrinsic pathway of apoptosis. Let us comment that RT-MLPA does not distinguish between the mRNAs coding for α and β isoforms and quantifies them together. To better understand the role of PUMA in our experimental paradigm, we distinguished both isoforms in the Western blot. We employed an anti-

PUMA polyclonal antibody able to recognize one band at 23-24 kDa (PUMA α) and another one at 16-18 kDa (PUMA β). The kinetic profile for PUMA α increase reproduced the profile of p53 stabilization, either at sublethal or at lethal concentrations of roscovitine (Fig. 5). The kinetic profile for PUMA β only reproduced the one of p53 in the sublethal treatment. At lethal concentrations of roscovitine, PUMA β displayed a tendency to decrease in a quite variable way (Fig. 5). Taken together these results agreed with our previous ones connecting p53 activation by roscovitine and the rise of *PUMA* mRNA. Moreover, we realized that the sum of PUMA α and β isoforms in the sublethal paradigm surpassed the sum in the lethal one. This provides an additional argumentation to support the lack of correlation between roscovitine-induced apoptosis and the increment of *PUMA* mRNA or PUMA α protein.

Finally, we focused on MCL-1, BCL-2 and BCL-X_L proteins (Fig. 6). BCL-2 and BCL-X_L protein content underwent decreases, but no clear difference emerged when sublethal and lethal conditions were compared. On the other hand, MCL-1 behaved quite differently. MCL-1 protein content increased at sublethal roscovitine concentrations and dramatically decreased at lethal ones. Consequently, the RT-MLPA results suggesting the depletion of MCL-1 as the best correlation for apoptosis induction seemed to be confirmed. If not discarded, the role for BCL-2 and BCL-X_L reduction in apoptosis induction seemed, at best, accessory.

Discussion

The experiments reported herein show that the cellular content of most mRNAs decay at 6 hours following a treatment with CDK inhibitory drugs, a time characterized by a minimal activity of effector caspases and, therefore, no loss of cell and mRNA integrity. This fact is consistent with the reported inhibition of CDK7 and CDK9 by this type of compounds [2, 26]. Respectively, CDK7 and CDK9 are essential elements in regulating transcription initiation and elongation by RNA polymerase II [26]. In other words, roscovitine and their analogues cause an early and marked reduction in the cellular

content of mRNAs due to a specific type of transcription inhibition. However, some genes are able to escape from this repression scenario. Precisely, we have found the *PUMA* mRNA to do so. PUMA is the acronym of p53-upregulated modulator of apoptosis. Accordingly, we have demonstrated this increase to be a transcriptional event mediated by p53. In addition, we have shown the mRNA increase to translate into increases of both, PUMA α and β proteins. Other p53-regulated genes can probably behave like *PUMA*. For instance, p21 protein is known to accumulate upon roscovitine treatment of SH-SY5Y cells [19]. The induction of *PUMA* and reduction of *MCL-1* expression are found in leukemic cells overexpressing protein $p16^{INK4A}$, a physiological inhibitor of CDK [27]. Moreover, our results closely mimic those reported for DRB (5,6-di-chloro-1-b-D-ribofuranosyl-benzimidazole), the most accepted chemical inhibitor of transcription elongation. Like roscovitine, DRB elicits p53 activation and promotes the expression of *p21* and *PUMA* genes in a context of broad transcription inhibition [28]. These opposing effects on transcription provide a good explanation for a paradoxical issue, the fact that roscovitine displays the ability to either induce [2] or prevent apoptosis [11, 12]. The roscovitine-induced modulation of the balance between apoptotic and antiapoptotic proteins provides a good explanation for it. If one protein required for apoptosis to occur is down-regulated, roscovitine will prevent apoptosis. On the contrary, apoptosis will take place if the down-regulated protein is antiapoptotic and necessary to keep a primed apoptosis in check. The molecular mechanisms explaining why some p53-regulated genes circumvent the disruption of transcription elongation by RNA polymerase II remain unclear and, in our opinion, deserve future investigations. Particularly, since these mechanisms seem to define a p53-mediated safeguard present in the cells to confront dysfunction in the process of transcription elongation.

On the other hand, we have shown that the up-regulation of *PUMA* is not a necessary event for roscovitine to induce apoptosis. We believe that the evidences obtained make unproductive additional experiments approaching this issue. Other events must happen and become more pivotal in the cell death process. For example, the marked reduction detected in the antiapoptotic MCL-1

protein. This result was not unexpected since it is the most agreed event in the mode of apoptosis induction by roscovitine [29-31]. However, some issues remained to be explained. Based on the existing knowledge, MCL-1 is expected to act by neutralizing one or several BH3-only proteins [25]. The question was which ones were being released following the MCL-1 decay and became the activators of apoptosis. Initially, PUMA protein was a good candidate. However, as stated before, our results concluded its role to be non-essential or, at best, supplementary. We knew that the overexpression of functional BCL-2 and BCL-X_L proteins do not protect SH-SY5Y cells from roscovitine [9]. Therefore, the BH-3 protein candidate should circumvent the neutralization of BCL-2 and BCL-X_L neutralization but not the one of MCL-1. This reasoning attracted our attention on NOXA, a BH3-only protein characterized by its specificity for MCL-1 interaction. Disappointingly, the RT-MLPA analyses were not informative since *NOXA* and *MCL-1* mRNA were found to decrease. Interestingly, when the protein content was characterized, we realized that NOXA did not decrease to the same extent than MCL-1. If Fig. 5 and 6 are compared, after 9-12 hours of roscovitine treatment, we will see MCL-1 has reduced its content eight times while NOXA has decreased, at best, one half. We propose this unbalance to be a decisive event in the mode of apoptosis induction by roscovitine. An analogous conclusion has been obtained in our previous reports about the apoptotic mode of action of NSAID (non-steroidal anti-inflammatory drugs) and Akt inhibitory compounds [32, 33]. Moreover, NOXA downregulation by RNA interference conferred a significant protection to hematological cell lines treated with seliciclib [34]. The decrease of MCL-1 protein is characteristic of apoptotic models caused by the inhibition of new protein synthesis [35-37]. The MCL-1 decay is the expected consequence of the proteosome avidity for MCL-1 digestion, which determines the elevated turnover of this protein. Consequently, the cellular MCL-1 content is a sensitive marker of the disruption of the transcriptional or translational machinery and the MCL-1/NOXA balance becomes the ideal rheostat to connect this dysfunction to apoptosis. While this report was in the reviewing process, NOXA was reported to be a substrate of CDK5. Upon

phosphorylation by CDK5 at serine 13, NOXA is sequestered in a cytosolic macromolecular complex and, as a consequence, its proapoptotic function at mitochondria is neutralized. [38]. In other words, not only the protein content of NOXA has to be taken into account but its phosphorylation state too. Roscovitine is a potent inhibitor of CDK5. Therefore, in our paradigm, NOXA will be hypophosphorylated. This means that the functional MCL-1/NOXA imbalance will be far greater than we suspected.

Finally, the just mentioned report introduces a new point to be discussed [38]. Which CDK entities have a relevant role in the apoptotic mode of action of Roscovitine? Roscovitine inhibits CDK1, 2, 5, 7 and 9 but not the other CDK [1]. Other kinases like ERK and pyridoxal kinase are inhibited by Roscovitine, but their involvement in our models has been discarded [9, 39]. It is now evident that the interplay of CDK5, CDK7 and CDK9 is crucial in establishing the ratio MCL-1/hypophosphorylated NOXA, the actual rheostat that will determine if apoptosis will occur. The role of CDK2 inhibition seems to be at best accessory, since cells defective in CDK2 display only a negligible death resistance when treated with Roscovitine [39]. Only the role of CDK1 in the apoptotic mode of action of Roscovitine remains to be ascertained. Since cells defective in CDK1 are not viable, a cellular model is lacking to address this issue.

Acknowledgements

J. Boix thanks F.I.S., "Instituto de Salud Carlos III", Spain (Project PI070498). Joan Gil thanks the "Ministerio de Ciencia e Innovación" and FEDER (SAF2010-20519), the "Instituto de Salud Carlos III" (RETIC RD06/0020) and the AGAUR-Generalitat de Catalunya (2009SGR-00395) for financial support. X.Garrofé-Ochoa was a pre-doctoral fellow from CUR-DIUE, Generalitat de Catalunya-European Social Fund.

Conflict of interest

The authors declare that they have no conflict of interest.

References

1. Knockaert M, Greengard P, Meijer L (2002) Pharmacological inhibitors of cyclin-dependent kinases. Trends Pharmacol Sci 23:417-425

2. Aldoss IT, Tashi T, Ganti AK (2009) Seliciclib in malignancies. Expert Opin Investig Drugs 18:1957-1965

3. Benson C, White J, De Bono J, O'Donnell A, Raynaud F, Cruickshank C, McGrath H, Walton M, Workman P, Kaye S, Cassidy J, Gianella-Borradori A, Judson I, Twelves C (2007) A phase I trial of the selective oral cyclin-dependent kinase inhibitor seliciclib (CYC202; R-Roscovitine), administered twice daily for 7 days every 21 days. Br J Cancer 96:29-37

4. Hsieh WS, Soo R, Peh BK, Loh T, Dong D, Soh D, Wong LS, Green S, Chiao J, Cui CY, Lai YF, Lee SC, Mow B, Soong R, Salto-Tellez M, Goh BC (2009) Pharmacodynamic effects of seliciclib, an orally administered cell cycle modulator, in undifferentiated nasopharyngeal cancer. Clin Cancer Res 15:1435-1442

5. Bettayeb K, Oumata N, Echalier A, Ferandin Y, Endicott JA, Galons H, Meijer L (2008) CR8, a potent and selective, roscovitine-derived inhibitor of cyclin-dependent kinases. Oncogene 27:5797-5807

6. Bettayeb K, Sallam H, Ferandin Y, Popowycz F, Fournet G, Hassan M, Echalier A, Bernard P, Endicott J, Joseph B, Meijer L (2008) N-&-N, a new class of cell death-inducing kinase inhibitors derived from the purine roscovitine. Mol Cancer Ther 7:2713-2724

7. Wesierska-Gadek J, Gueorguieva M, Kramer MP, Ranftler C, Sarg B, Lindner H (2007) A new, unexpected action of olomoucine, a CDK inhibitor, on normal human cells: up-regulation of CLIMP-63, a cytoskeleton-linking membrane protein. J Cell Biochem 102:1405-1419

8. Vesely J, Havlicek L, Strnad M, Blow JJ, Donella-Deana A, Pinna L, Letham DS, Kato J, Detivaud L, Leclerc S, et al. (1994) Inhibition of cyclin-dependent kinases by purine analogues. Eur J Biochem 224:771-786

9. Ribas J, Boix J (2004) Cell differentiation, caspase inhibition, and macromolecular synthesis blockage, but not BCL-2 or BCL-XL proteins, protect SH-SY5Y cells from apoptosis triggered by two CDK inhibitory drugs. Exp Cell Res 295:9-24

10. Leitch AE, Riley NA, Sheldrake TA, Festa M, Fox S, Duffin R, Haslett C, Rossi AG (2010) The cyclin-dependent kinase inhibitor R-roscovitine down-regulates Mcl-1 to override pro-inflammatory signalling and drive neutrophil apoptosis. Eur J Immunol 40:1127-1138

11. Hakem A, Sasaki T, Kozieradzki I, Penninger JM (1999) The cyclin-dependent kinase Cdk2 regulates thymocyte apoptosis. J Exp Med 189:957-968

12. Padmanabhan J, Park DS, Greene LA, Shelanski ML (1999) Role of cell cycle regulatory proteins in cerebellar granule neuron apoptosis. J Neurosci 19:8747-8756

13. Ribas J, Gomez-Arbones X, Boix J (2005) Caspase 8/10 are not mediating apoptosis in neuroblastoma cells treated with CDK inhibitory drugs. Eur J Pharmacol 524:49-52

14. Garrofe-Ochoa X, Melero-Fernandez de Mera RM, Fernandez-Gomez FJ, Ribas J, Jordan J, Boix J (2008) BAX and BAK proteins are required for cyclin-dependent kinase inhibitory drugs to cause apoptosis. Mol Cancer Ther 7:3800-3806

15. Eldering E, Spek CA, Aberson HL, Grummels A, Derks IA, de Vos AF, McElgunn CJ, Schouten JP (2003) Expression profiling via novel multiplex assay allows rapid assessment of gene regulation in defined signalling pathways. Nucleic Acids Res 31:e153

16. Coll-Mulet L, Iglesias-Serret D, Santidrian AF, Cosialls AM, de Frias M, Castano E, Campas C, Barragan M, de Sevilla AF, Domingo A, Vassilev LT, Pons G, Gil J (2006) MDM2 antagonists activate p53 and synergize with genotoxic drugs in B-cell chronic lymphocytic leukemia cells. Blood 107:4109-4114

17. Boix J, Llecha N, Yuste VJ, Comella JX (1997) Characterization of the cell death process induced by staurosporine in human neuroblastoma cell lines. Neuropharmacology 36:811-821

18. Yuste VJ, Bayascas JR, Llecha N, Sanchez-Lopez I, Boix J, Comella JX (2001) The absence of oligonucleosomal DNA fragmentation during apoptosis of IMR-5 neuroblastoma cells: disappearance of the caspase-activated DNase. J Biol Chem 276:22323-22331

19. Ribas J, Boix J, Meijer L (2006) (R)-roscovitine (CYC202, Seliciclib) sensitizes SH-SY5Y neuroblastoma cells to nutlin-3-induced apoptosis. Exp Cell Res 312:2394-2400

20. Yu J, Zhang L, Hwang PM, Kinzler KW, Vogelstein B (2001) PUMA induces the rapid apoptosis of colorectal cancer cells. Mol Cell 7:673-682

21. Nakano K, Vousden KH (2001) PUMA, a novel proapoptotic gene, is induced by p53. Mol Cell 7:683-694

22. Wolf D, Rotter V (1985) Major deletions in the gene encoding the p53 tumor antigen cause lack of p53 expression in HL-60 cells. Proc Natl Acad Sci U S A 82:790-794

23. Cheng J, Haas M (1990) Frequent mutations in the p53 tumor suppressor gene in human leukemia T-cell lines. Mol Cell Biol 10:5502-5509

24. Komarov PG, Komarova EA, Kondratov RV, Christov-Tselkov K, Coon JS, Chernov MV, Gudkov AV (1999) A chemical inhibitor of p53 that protects mice from the side effects of cancer therapy. Science 285:1733-1737

25. Chipuk JE, Moldoveanu T, Llambi F, Parsons MJ, Green DR (2010) The BCL-2 family reunion. Mol Cell 37:299-310

26. Wang S, Fischer PM (2008) Cyclin-dependent kinase 9: a key transcriptional regulator and potential drug target in oncology, virology and cardiology. Trends Pharmacol Sci 29:302-313

27. Obexer P, Hagenbuchner J, Rupp M, Salvador C, Holzner M, Deutsch M, Porto V, Kofler R, Unterkircher T, Ausserlechner MJ (2009) p16INK4A sensitizes human leukemia cells to FAS- and

glucocorticoid-induced apoptosis via induction of BBC3/Puma and repression of MCL1 and BCL2. J Biol Chem 284:30933-30940

28. Gomes NP, Bjerke G, Llorente B, Szostek SA, Emerson BM, Espinosa JM (2006) Gene-specific requirement for P-TEFb activity and RNA polymerase II phosphorylation within the p53 transcriptional program. Genes Dev 20:601-612

29. Alvi AJ, Austen B, Weston VJ, Fegan C, MacCallum D, Gianella-Borradori A, Lane DP, Hubank M, Powell JE, Wei W, Taylor AM, Moss PA, Stankovic T (2005) A novel CDK inhibitor, CYC202 (R-roscovitine), overcomes the defect in p53-dependent apoptosis in B-CLL by down-regulation of genes involved in transcription regulation and survival. Blood 105:4484-4491

30. MacCallum DE, Melville J, Frame S, Watt K, Anderson S, Gianella-Borradori A, Lane DP, Green SR (2005) Seliciclib (CYC202, R-Roscovitine) induces cell death in multiple myeloma cells by inhibition of RNA polymerase II-dependent transcription and down-regulation of Mcl-1. Cancer Res 65:5399-5407

31. Raje N, Kumar S, Hideshima T, Roccaro A, Ishitsuka K, Yasui H, Shiraishi N, Chauhan D, Munshi NC, Green SR, Anderson KC (2005) Seliciclib (CYC202 or R-roscovitine), a small-molecule cyclin-dependent kinase inhibitor, mediates activity via down-regulation of Mcl-1 in multiple myeloma. Blood 106:1042-1047

32. de Frias M, Iglesias-Serret D, Cosialls AM, Coll-Mulet L, Santidrian AF, Gonzalez-Girones DM, de la Banda E, Pons G, Gil J (2009) Akt inhibitors induce apoptosis in chronic lymphocytic leukemia cells. Haematologica 94:1698-1707

33. Iglesias-Serret D, Pique M, Barragan M, Cosialls AM, Santidrian AF, Gonzalez-Girones DM, Coll-Mulet L, de Frias M, Pons G, Gil J (2010) Aspirin induces apoptosis in human leukemia cells independently of NF-kappaB and MAPKs through alteration of the Mcl-1/Noxa balance. Apoptosis 15:219-229

34. Hallaert DY, Spijker R, Jak M, Derks IA, Alves NL, Wensveen FM, de Boer JP, de Jong D, Green SR, van Oers MH, Eldering E (2007) Crosstalk among Bcl-2 family members in B-CLL: seliciclib acts via the Mcl-1/Noxa axis and gradual exhaustion of Bcl-2 protection. Cell Death Differ 14:1958-1967

35. Cuconati A, Mukherjee C, Perez D, White E (2003) DNA damage response and MCL-1 destruction initiate apoptosis in adenovirus-infected cells. Genes Dev 17:2922-2932

36. Nijhawan D, Fang M, Traer E, Zhong Q, Gao W, Du F, Wang X (2003) Elimination of Mcl-1 is required for the initiation of apoptosis following ultraviolet irradiation. Genes Dev 17:1475-1486

37. Rahmani M, Davis EM, Bauer C, Dent P, Grant S (2005) Apoptosis induced by the kinase inhibitor BAY 43-9006 in human leukemia cells involves down-regulation of Mcl-1 through inhibition of translation. J Biol Chem 280:35217-35227

38. Lowman XH, McDonnell MA, Kosloske A, Odumade OA, Jenness C, Karim CB, Jemmerson R, Kelekar A (2010) The proapoptotic function of Noxa in human leukemia cells is regulated by the kinase Cdk5 and by glucose. Mol Cell 40:823-833

39. Bach S, Knockaert M, Reinhardt J, Lozach O, Schmitt S, Baratte B, Koken M, Coburn SP, Tang L, Jiang T, Liang DC, Galons H, Dierick JF, Pinna LA, Meggio F, Totzke F, Schachtele C, Lerman AS, Carnero A, Wan Y, Gray N, Meijer L (2005) Roscovitine targets, protein kinases and pyridoxal kinase. J Biol Chem 280:31208-31219

Figure legends

Fig. 1. Expression profile of apoptosis-related genes in SH-SY5Y cells treated with roscovitine. After 6 hours of treatment, roscovitine (50 µM) modified the mRNA content of 29 genes involved in apoptosis regulation. Data were obtained by the RT-MLPA procedure. Gene name and classification are indicated at the bottom of the figure (x axis). Quantification of mRNA (y axis) is expressed as the

base-2 logarithm (log2) of the fold induction relative to untreated SH-SY5Y cells. Values are the mean ± S.E.M. of 5 independent experiments.

Fig. 2. Comparative analyses performed by RT-MLPA. A, SH-SY5Y cells were treated for 6 hours with 200 μM olomoucine (black bars), 200 μM iso-olomoucine (white bars) and 50 μM seliciclib (grey bars). B, human neuroblastoma cell lines IMR-5 (black bars) and IMR-32 (grey bars) were treated with 50 μM roscovitine for 6 h. Axes in the diagrams are defined as in previous Fig. 1.

Fig. 3. Effects of roscovitine treatment on cell lines defective in p53. A, HL-60 (black bars) and Jurkat (white bars) cells were treated for 24 hours with increasing concentrations of roscovitine (x axis). Cell viability was measured by the MTS reduction procedure. Bar value is the mean ± S.E.M. of 3 experiments (**P*<0.01, Student's t-test referred to the untreated value). B, HL-60 (black bars) and Jurkat (white bars) cells were treated for 48 hours with increasing concentrations of roscovitine (x axis). Cell death was measured by determining the released percentage of total LDH. Values are mean ± S.E.M. of 3 experiments (**P*< 0.01, Student's t-test referred to the untreated value). C, HL-60 and Jurkat cells were treated for 24 hours with roscovitine (50 μM) and the activation of effector caspases quantified by the coumarin fluorescence released from a substrate (N-acetyl-DEVD-7-amido-4-trifluoromethylcoumarin). Basal values of untreated cells are also displayed (grey bars). DEVDase activity is measured in arbitrary fluorescent units (a.f.u.). Values are the mean ± S.E.M. of 4 experiments (**P*< 0.01, Student's t-test referred to the basal value). D, HL-60 (black bars) and Jurkat (white bars) cells were treated for 6 hours with roscovitine (50 μM) and subjected to RT-MLPA analysis as in the previous figures.

Fig. 4. PUMA mRNA increase in SH-SY5Y cells was mediated by p53 and failed to correlate with cell death induction. A, Pft-α and cPft-α are two inhibitors of the p53 transcriptional activity. Cells

were treated for 6 hours with roscovitine (50 μM), Pft-α (30 μM), cPft-α (30 μM) and the combinations stated in the graph. Then, total RNA was extracted and subjected to RT-MLPA analysis. Only the effect on PUMA mRNA was significant and, therefore, is shown. The relative PUMA mRNA content (y axis) was calculated as described in the previous figures. B, cells were treated with roscovitine (50 μM), Pft-α (30 μM), cPft-α (30 μM) and the combinations stated in the graph. After 48 hours of treatment cell death was assessed by the LDH procedure as before. Bar values are the mean ± S.E.M. of 3 experiments performed in triplicate. C, the effects on the mRNA content of a sublethal versus a lethal concentration of roscovitine was compared. SH-SY5Y cells were treated for 6 hours with roscovitine at either 10 μM (grey bars, sublethal concentration) or 50 μM (black bars, lethal concentration). Total RNA was extracted and subjected to RT-MLPA analyses as before.

Fig. 5. Time course of p53, NOXA and PUMA protein content in SH-SY5Y cells treated with sublethal and lethal doses of roscovitine. SH-SY5Y cells were treated with roscovitine at either 10 μM (grey bars, sublethal concentration) or 50 μM (black bars, lethal concentration) for 3, 6, 9 and 12 hours (x axis). Proteins were extracted and analyzed by Western blot. Following quantification by densitometry, the fold induction was calculated for A, p53; B, NOXA; C, PUMA α; D, PUMA β. Values were expressed as a base-2 logarithm (y axis). Mean ± S.E.M. of 3 independent experiments are shown.

Fig. 6. Time course of MCL-1, BCL-2 and BCL-XL protein content in SH-SY5Y cells treated with sublethal and lethal doses of roscovitine. SH-SY5Y cells were treated with roscovitine at 10 μM (grey bars, sublethal concentration) or 50 μM (black bars, lethal concentration) for the time indicated (x axis). Proteins were extracted and analyzed by Western blot. Following quantification by densitometry, the fold induction was calculated for A, MCL-1; B, BCL-2; C, BCL-XL. Values are the mean ± S.E.M. of 3 independent experiments and are expressed as a base-2 logarithm.

Fig. 1.

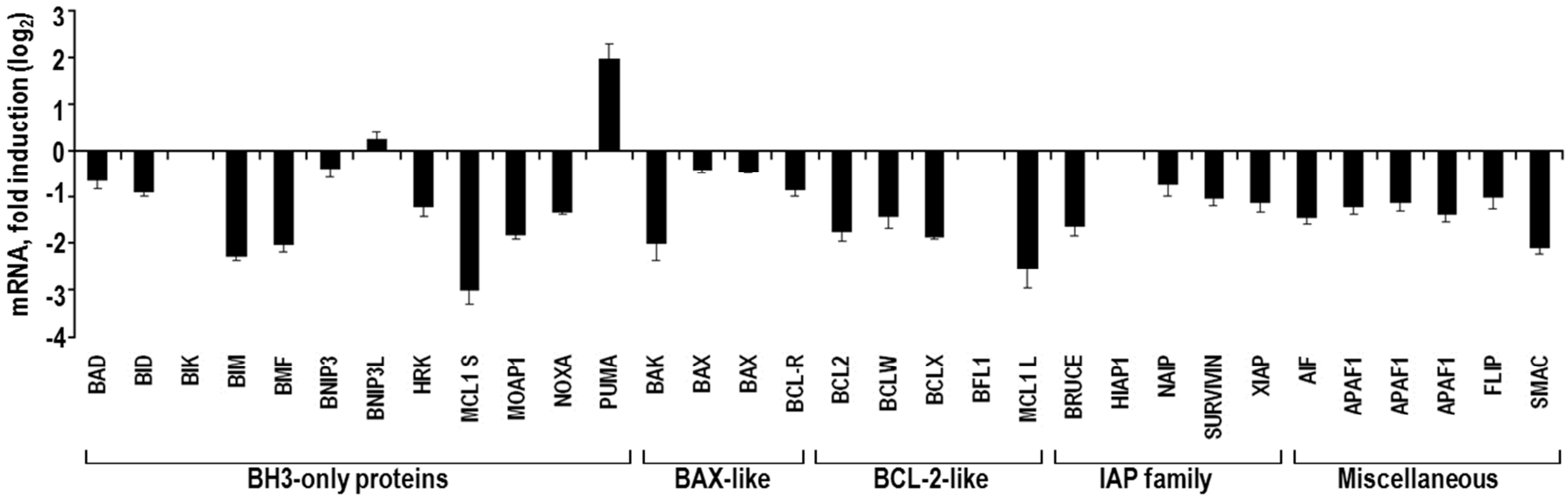
mRNA, fold induction (log2)
3
2
1
0
-1
-2
-3
-4
BAD
BID
BIK
BIM
BMF
BNIP3
BNIP3L
HRK
MCL1 S
MOAP1
NOXA
PUMA
BAK
BAX
BAX
BCL-R
BCL2
BCLW
BCLX
BFL1
MCL1 L
BRUCE
HIAP1
NAIP
SURVIVIN
XIAP
AIF
APAF1
APAF1
APAF1
FLIP
SMAC
BH3-only proteins
BAX-like
BCL-2-like
IAP family
Miscellaneous

Fig. 2.

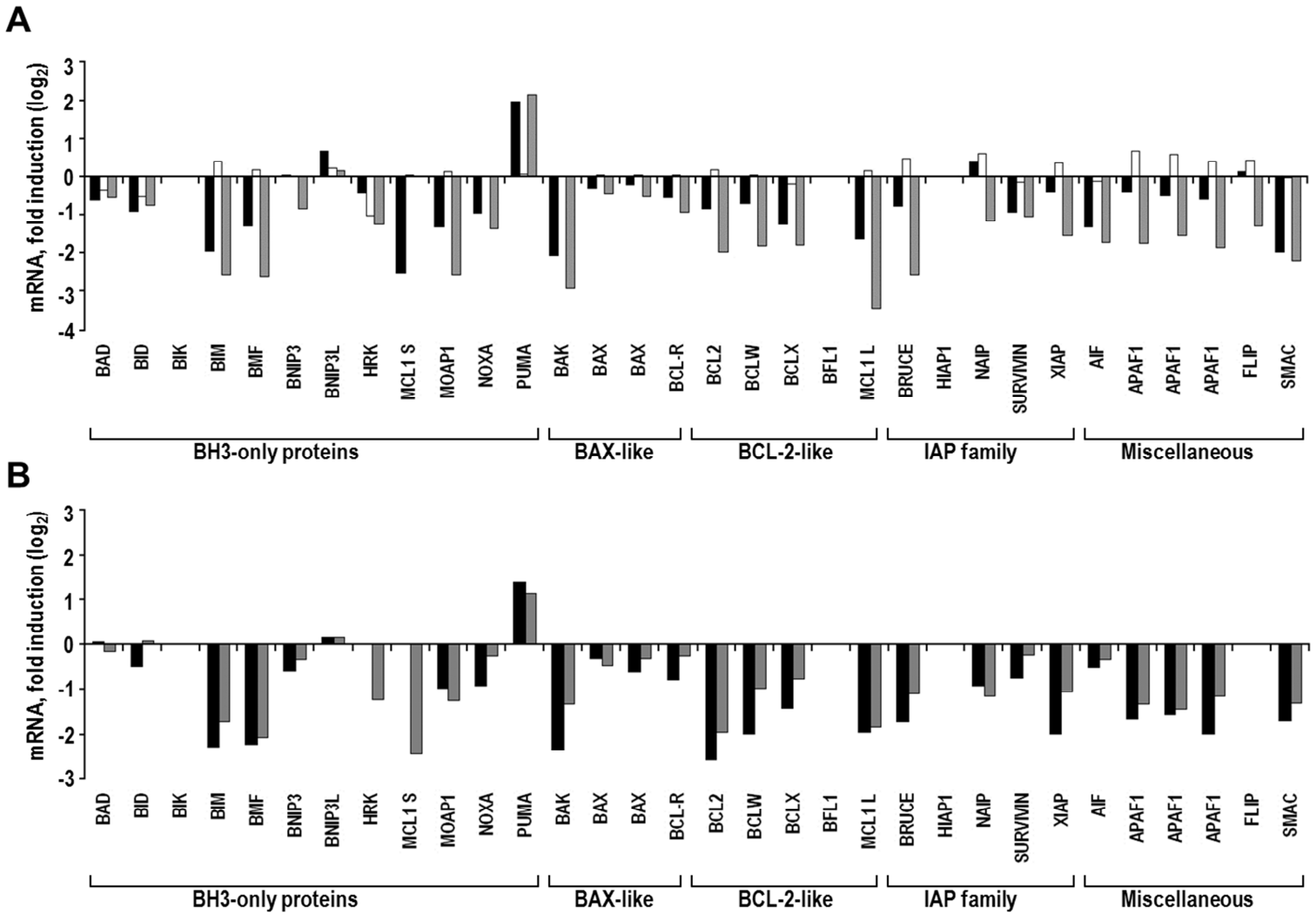
A
mRNA, fold induction (log2)
3
2
1
0
-1
-2
-3
-4
BAD
BID
BIK
BIM
BMF
BNIP3
BNIP3L
HRK
MCL1 S
MOAP1
NOXA
PUMA
BAK
BAX
BAX
BCL-R
BCL2
BCLW
BCLX
BFL1
MCL1 L
BRUCE
HIAP1
NAIP
SURVIVIN
XIAP
AIF
APAF1
APAF1
APAF1
FLIP
SMAC
BH3-only proteins
BAX-like
BCL-2-like
IAP family
Miscellaneous
B
mRNA, fold induction (log2)
3
2
1
0
-1
-2
-3
BAD
BID
BIK
BIM
BMF
BNIP3
BNIP3L
HRK
MCL1 S
MOAP1
NOXA
PUMA
BAK
BAX
BAX
BCL-R
BCL2
BCLW
BCLX
BFL1
MCL1 L
BRUCE
HIAP1
NAIP
SURVIVIN
XIAP
AIF
APAF1
APAF1
APAF1
FLIP
SMAC
BH3-only proteins
BAX-like
BCL-2-like
IAP family
Miscellaneous

Fig. 3.

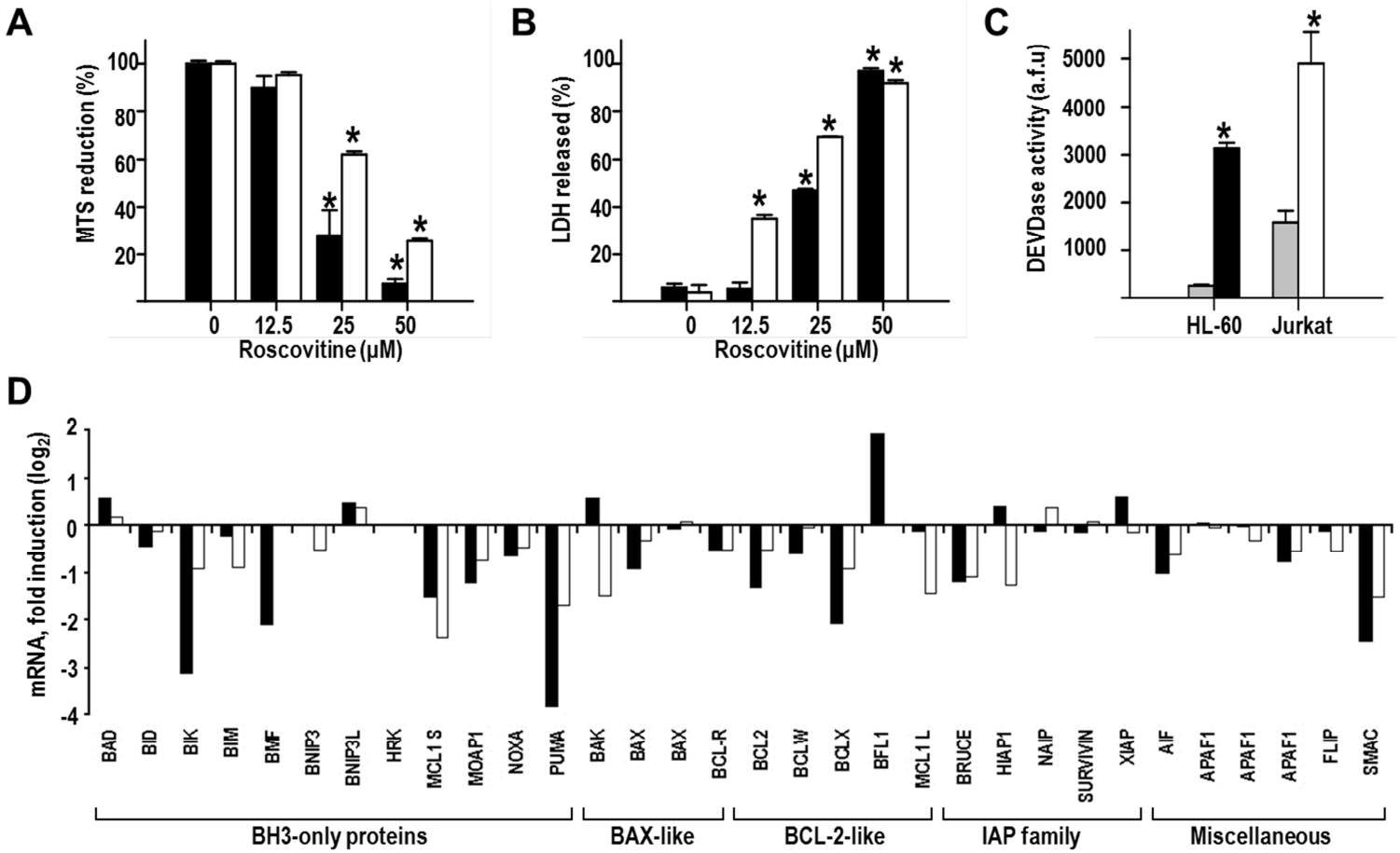
A
MTS reduction (%)
100
80
60
40
20
0
12.5
25
50
Roscovitine (μM)
B
LDH released (%)
100
80
60
40
20
0
12.5
25
50
Roscovitine (μM)
C
DEVDase activity (a.f.u)
5000
4000
3000
2000
1000
HL-60
Jurkat
D
mRNA, fold induction (log2)
2
1
0
-1
-2
-3
-4
BAD
BID
BIK
BIM
BMF
BNIP3
BNIP3L
HRK
MCL1 S
MOAP1
NOXA
PUMA
BAK
BAX
BAX
BCL-R
BCL2
BCLW
BCLX
BFL1
MCL1 L
BRUCE
HIAP1
NAIP
SURVIVIN
XIAP
AIF
APAF1
APAF1
APAF1
FLIP
SMAC
BH3-only proteins
BAX-like
BCL-2-like
IAP family
Miscellaneous

Fig. 4.

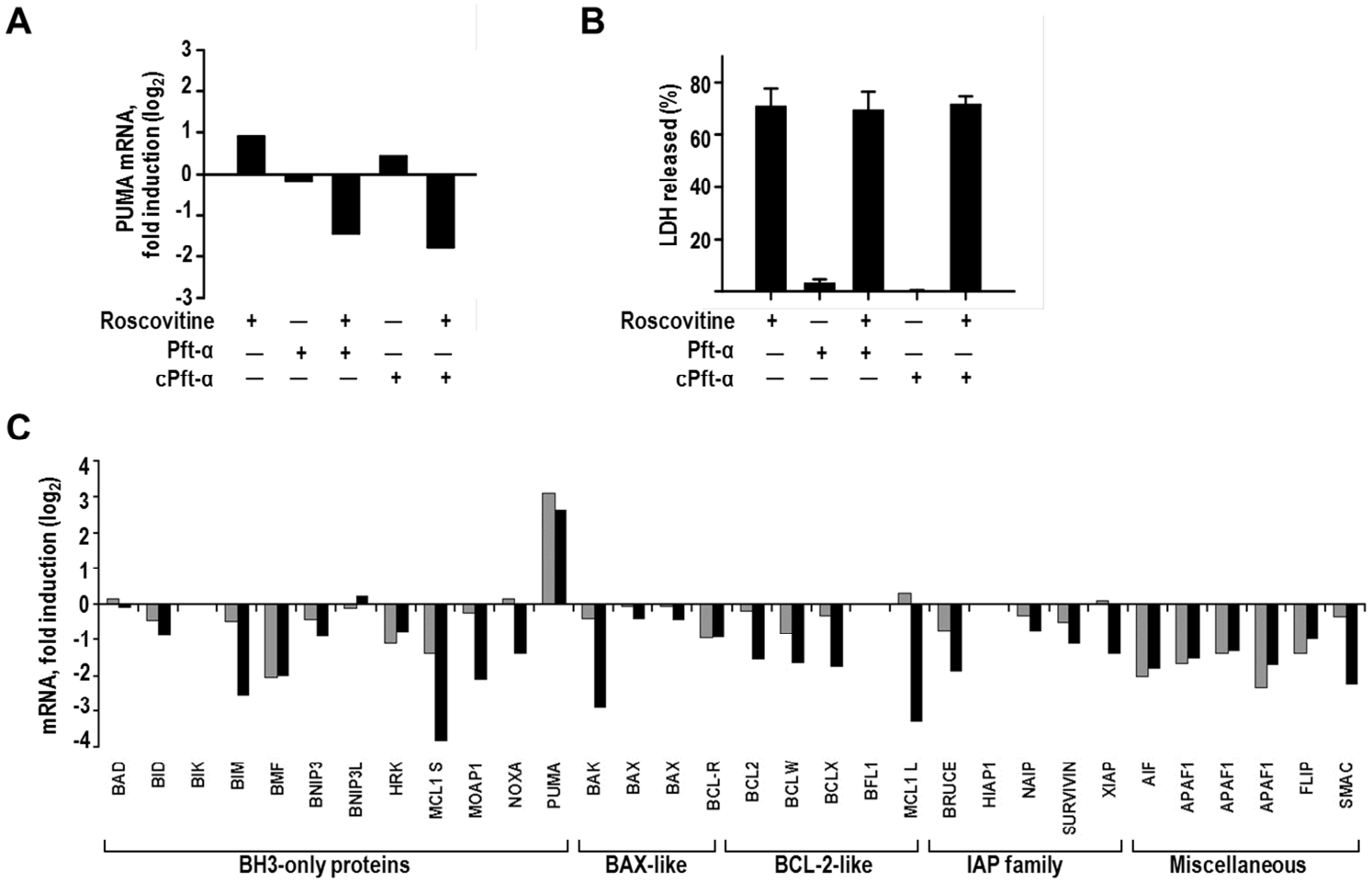
A
PUMA mRNA, fold induction (log2)
3
2
1
0
-1
-2
-3
Roscovitine + — + — +
Pft-α — + + — —
cPft-α — — — + +
B
LDH released (%)
80
60
40
20
Roscovitine + — + — +
Pft-α — + + — —
cPft-α — — — + +
C
mRNA, fold induction (log2)
4
3
2
1
0
-1
-2
-3
-4
BAD
BID
BIK
BIM
BMF
BNIP3
BNIP3L
HRK
MCL1 S
MOAP1
NOXA
PUMA
BAK
BAX
BAX
BCL-R
BCL2
BCLW
BCLX
BFL1
MCL1 L
BRUCE
HIAP1
NAIP
SURVIVIN
XIAP
AIF
APAF1
APAF1
APAF1
FLIP
SMAC
BH3-only proteins
BAX-like
BCL-2-like
IAP family
Miscellaneous

Fig. 5.

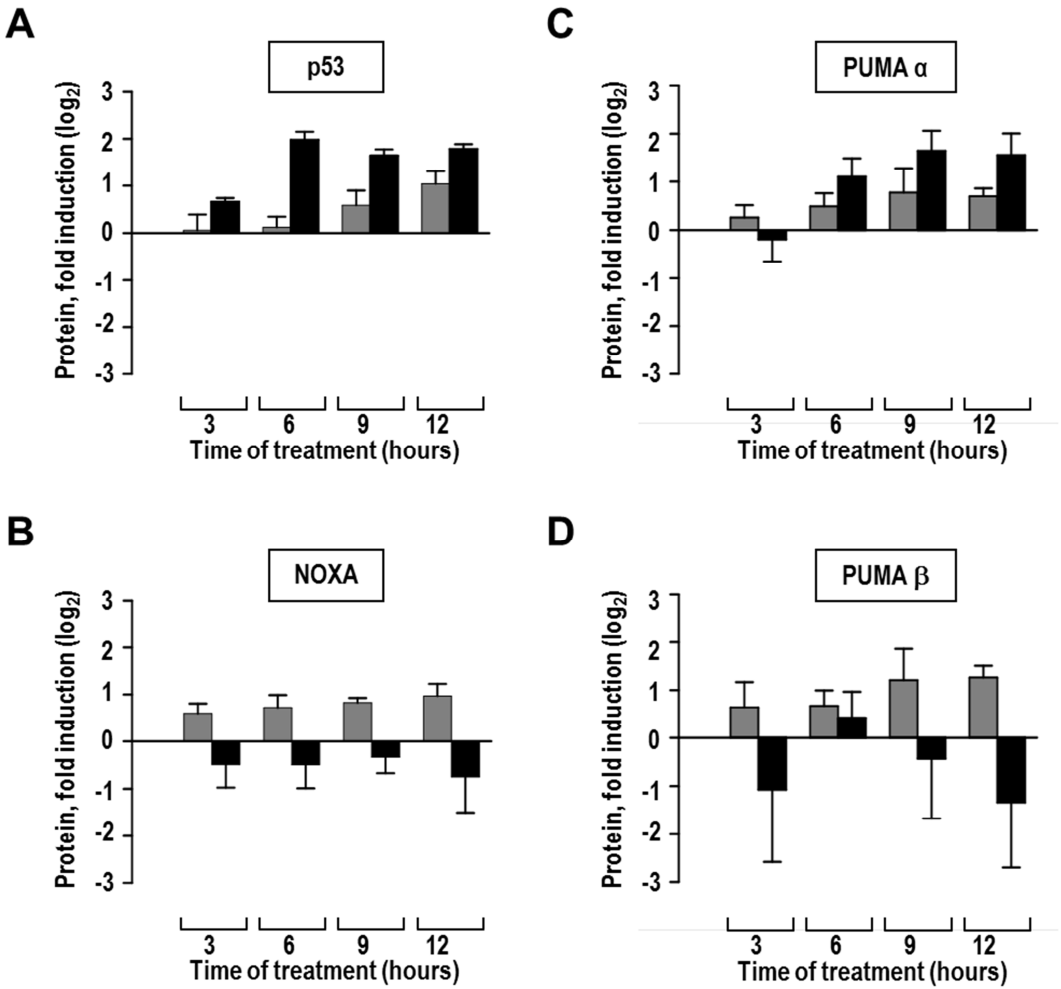
A
p53
Protein, fold induction (log2)
3
2
1
0
-1
-2
-3
3
6
9
12
Time of treatment (hours)
C
PUMA α
Protein, fold induction (log2)
3
2
1
0
-1
-2
-3
3
6
9
12
Time of treatment (hours)
B
NOXA
Protein, fold induction (log2)
3
2
1
0
-1
-2
-3
3
6
9
12
Time of treatment (hours)
D
PUMA β
Protein, fold induction (log2)
3
2
1
0
-1
-2
-3
3
6
9
12
Time of treatment (hours)

Fig. 6.

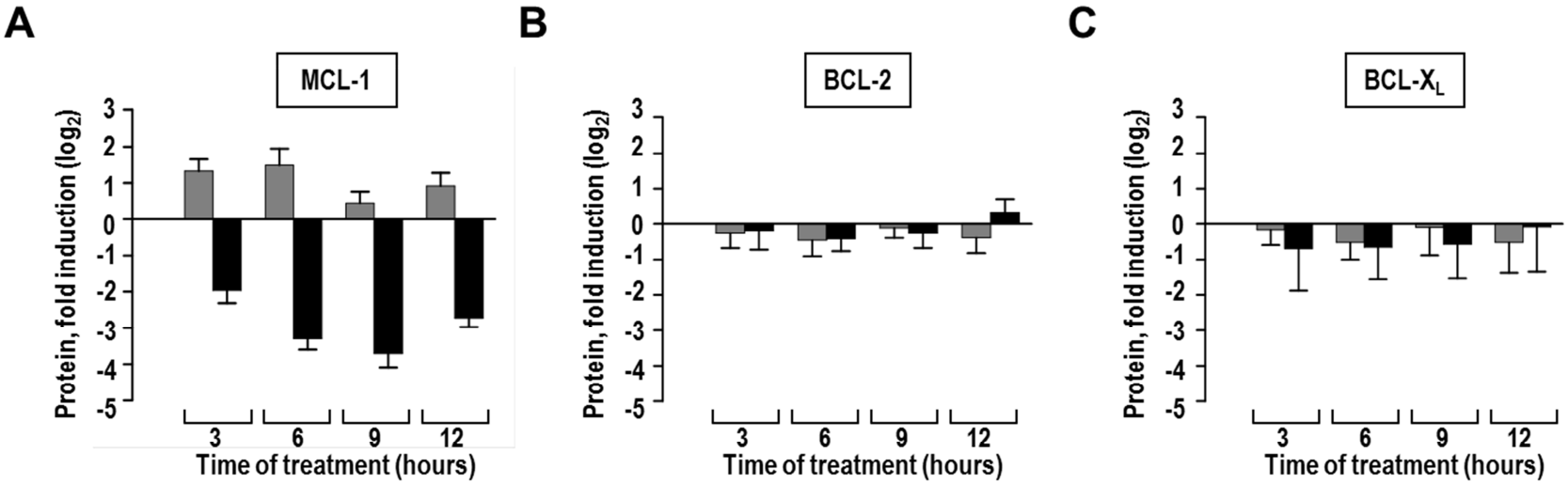
A
MCL-1
Protein, fold induction (log2)
3
2
1
0
-1
-2
-3
-4
-5
3
6
9
12
Time of treatment (hours)
B
BCL-2
Protein, fold induction (log2)
3
2
1
0
-1
-2
-3
-4
-5
3
6
9
12
Time of treatment (hours)
C
BCL-XL
Protein, fold induction (log2)
3
2
1
0
-1
-2
-3
-4
-5
3
6
9
12
Time of treatment (hours)

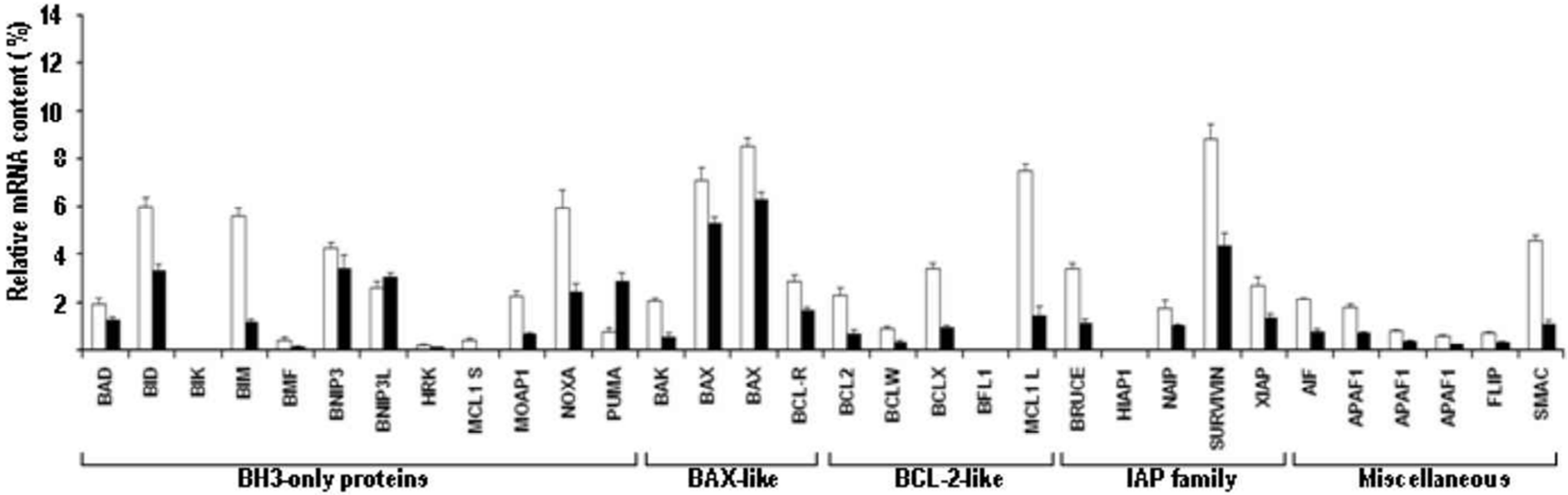

Supplemental Fig. 1

Expression profile of apoptosis-related genes in SH-SY5Y cells treated with roscovitine. After 6 hours of treatment, roscovitine (50 µM) modified the mRNA content of 29 genes involved in apoptosis regulation. Data were obtained by the RT-MLPA procedure. Gene name and classification are indicated at the bottom of the figure (x axis). This supplemental figure is based on the same data than Fig. 1. Here, mRNA expression levels of the treated condition (black bars) are not related to the untreated one (white bars). Although this representation provides a less visual display of the changes associated to drug treatment than the log2 option, it allows the assessment of the extent each gene is expressed by the cells. Values are the mean ± S.E.M. of 5 independent experiments.

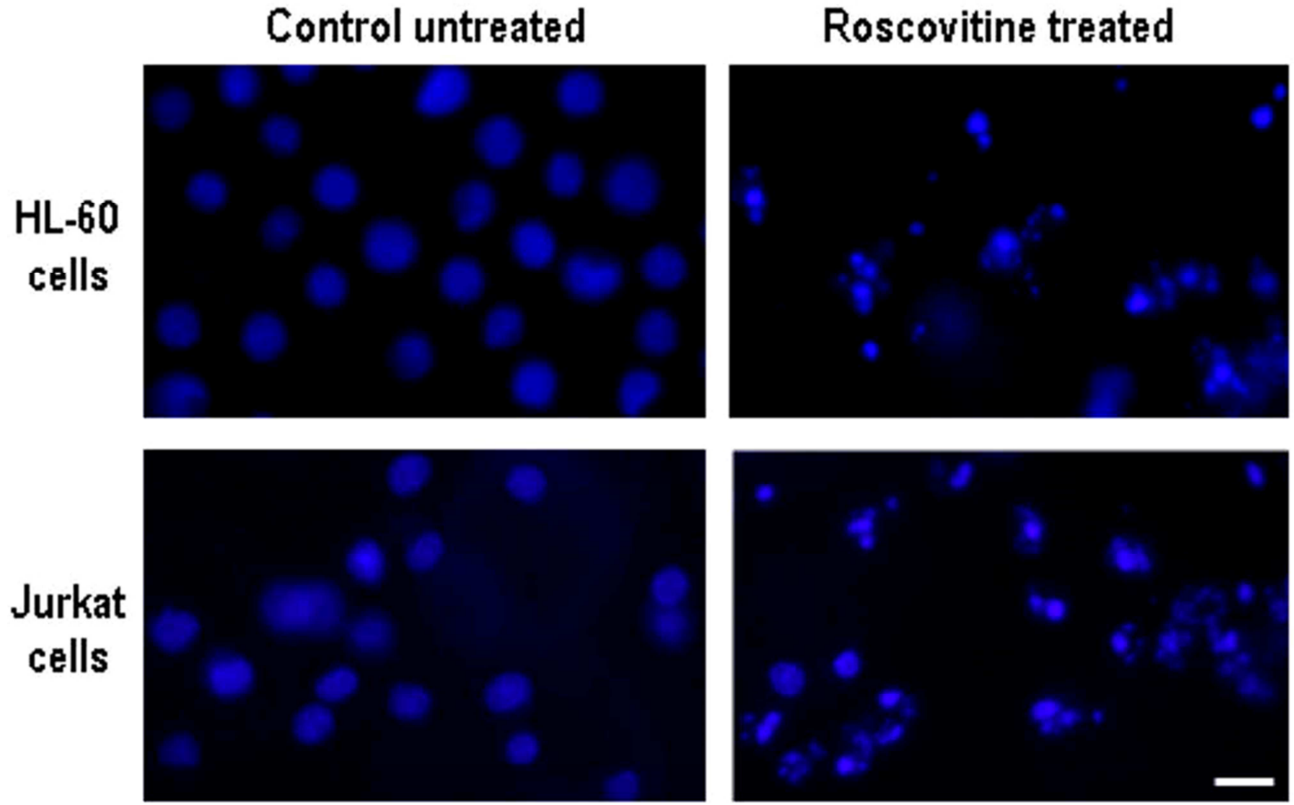

Supplemental Fig. 2

The cell lines stated in the image were treated with Roscovitine (50μM) for 24 hours or left untreated. Then cells were subjected to direct bisBenzimide staining and fluorescence microscopy. Bar = 10μM.

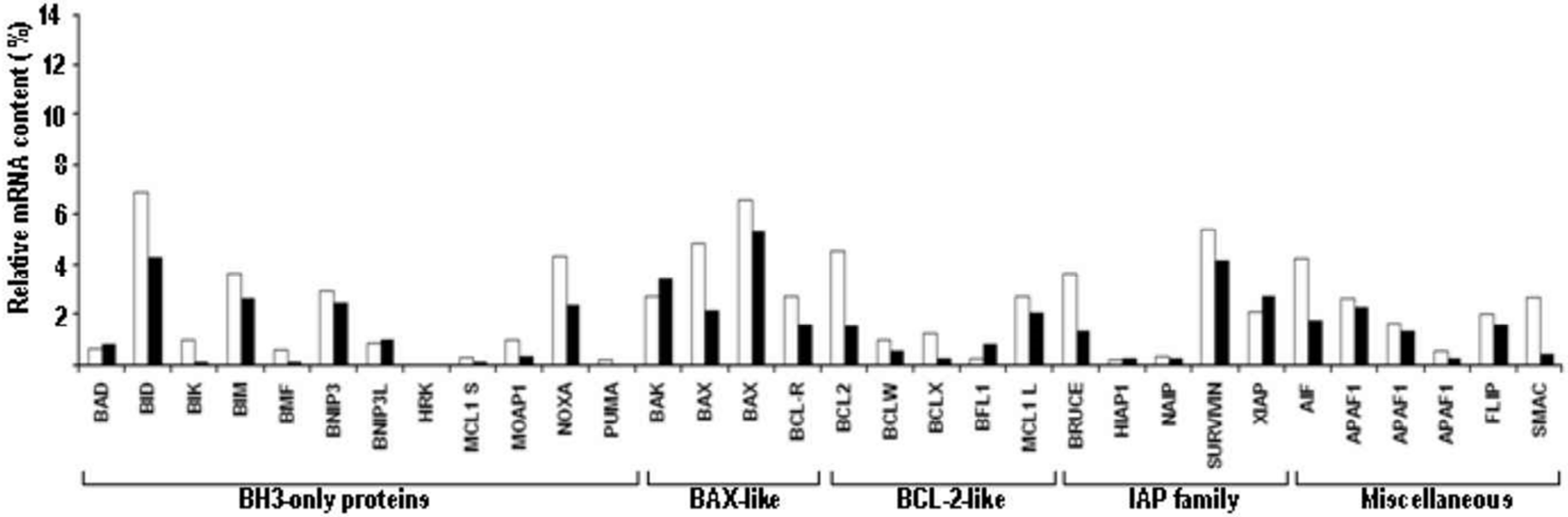

Supplemental Fig. 3

Expression profile of apoptosis-related genes in HL-60 cells treated with roscovitine. HL-60 cells were treated (black bars) for 6 hours with roscovitine (50 µM) or left untreated (white bars). Then total RNA was extracted and subjected to RT-MLPA analysis. This supplemental figure is based on identical data than Fig. 3D. However, the quantification of mRNA has been performed as reported in the legend of supplemental Fig. 1

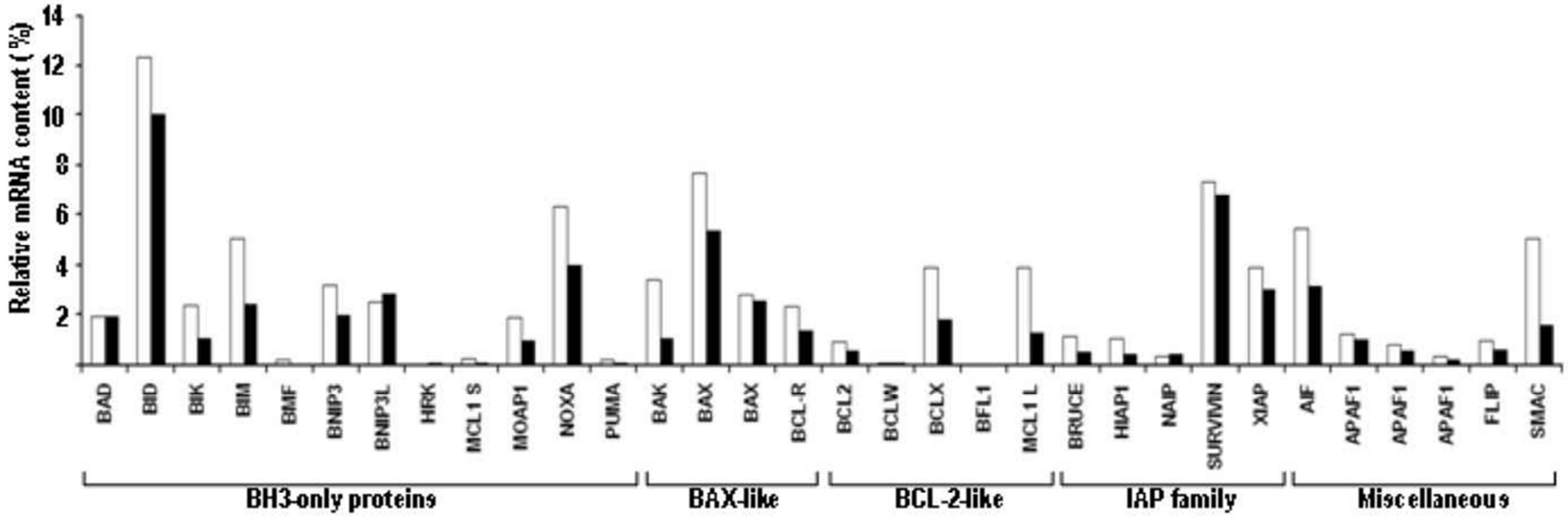

Supplemental Fig. 4

Expression profile of apoptosis-related genes in Jurkat cells treated with roscovitine. Jurkat cells were treated (black bars) for 6 hours with roscovitine (50 µM) or left untreated (white bars). Then total RNA was extracted and subjected to RT-MLPA analysis. This supplemental figure is based on identical data than Fig. 3D. However, the quantification of mRNA has been performed as reported in the legend of supplemental Fig. 1

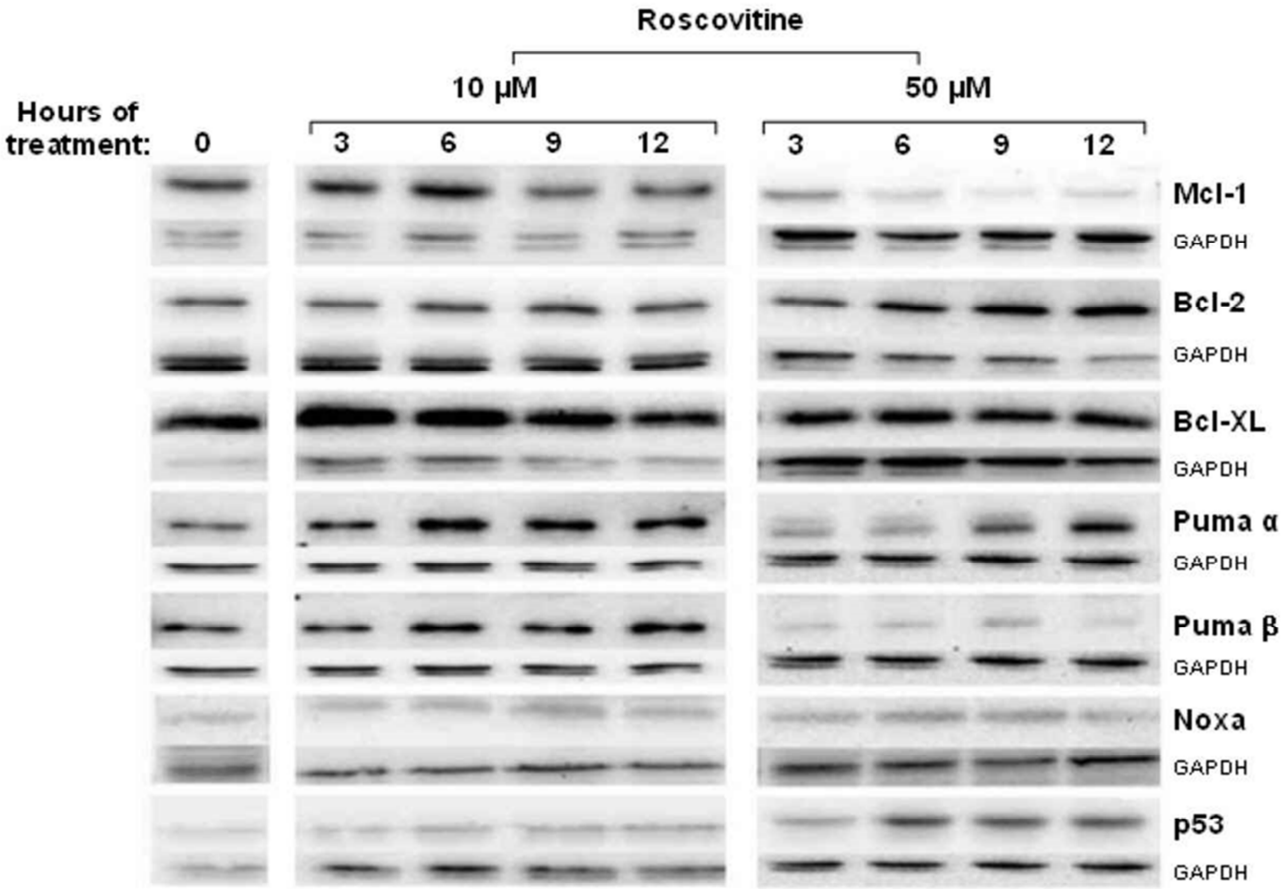

Supplemental Fig. 5

Western blot images representative of those processed by densitometry to generate Fig. 5 and 6. SH-SY5Y cells were treated with sublethal (10µM) and lethal (50µM) concentrations of roscovitine for the time stated in the image. Then proteins extracts were performed and subjected to Western blot to analyze the content of the proteins indicated in the image. GAPDH was used to assess the amount of protein loaded per lane.